



TITLE:

# Long-Term Outcome of Sciatic Nerve Regeneration Using Bio3D Conduit Fabricated from Human Fibroblasts in a Rat Sciatic Nerve Model

AUTHOR(S):

Ando, Maki; Ikeguchi, Ryosuke; Aoyama, Tomoki; Tanaka, Mai; Noguchi, Takashi; Miyazaki, Yudai; Akieda, Shizuka; Nakayama, Koichi; Matsuda, Shuichi

---

CITATION:

Ando, Maki ...[et al]. Long-Term Outcome of Sciatic Nerve Regeneration Using Bio3D Conduit Fabricated from Human Fibroblasts in a Rat Sciatic Nerve Model. Cell Transplantation 2021, 30

ISSUE DATE:

2021


URL:

<http://hdl.handle.net/2433/277001>

RIGHT:

© The Author(s) 2021.; This article is distributed under the terms of the Creative Commons Attribution-NonCommercial 4.0 License which permits non-commercial use, reproduction and distribution of the work without further permission provided the original work is attributed as specified on the SAGE and Open Access pages (<https://us.sagepub.com/en-us/nam/open-access-at-sage>).

# Long-Term Outcome of Sciatic Nerve Regeneration Using Bio3D Conduit Fabricated from Human Fibroblasts in a Rat Sciatic Nerve Model

Cell Transplantation  
Volume 30: 1–12  
© The Author(s) 2021  
Article reuse guidelines:  
[sagepub.com/journals-permissions](https://sagepub.com/journals-permissions)  
DOI: 10.1177/09636897211021357  
[journals.sagepub.com/home/cll](https://journals.sagepub.com/home/cll)  


Maki Ando, Ryosuke Ikeguchi , Tomoki Aoyama, Mai Tanaka, Takashi Noguchi, Yudai Miyazaki, Shizuka Akieda, Koichi Nakayama , and Shuichi Matsuda

## Abstract

Previously, we developed a Bio3D conduit fabricated from human fibroblasts and reported a significantly better outcome compared with artificial nerve conduit in the treatment of rat sciatic nerve defect. The purpose of this study is to investigate the long-term safety and nerve regeneration of Bio3D conduit compared with treatments using artificial nerve conduit and autologous nerve transplantation.

We used 15 immunodeficient rats and randomly divided them into three groups treated with Bio3D ( $n = 5$ ) conduit, silicon tube ( $n = 5$ ), and autologous nerve transplantation ( $n = 5$ ). We developed Bio3D conduits composed of human fibroblasts and bridged the 5 mm nerve gap created in the rat sciatic nerve. The same procedures were performed to bridge the 5 mm gap with a silicon tube. In the autologous nerve group, we removed the 5 mm sciatic nerve segment and transplanted it. We evaluated the nerve regeneration 24 weeks after surgery.

Toe dragging was significantly better in the Bio3D group ( $0.20 \pm 0.28$ ) than in the silicon group ( $0.6 \pm 0.24$ ). The wet muscle weight ratios of the tibial anterior muscle of the Bio3D group ( $79.85\% \pm 5.47\%$ ) and the autologous nerve group ( $81.74\% \pm 2.83\%$ ) were significantly higher than that of the silicon group ( $66.99\% \pm 3.51\%$ ). The number of myelinated axons and mean myelinated axon diameter was significantly higher in the Bio3D group ( $14708 \pm 302$  and  $5.52 \pm 0.44 \mu\text{m}$ ) and the autologous nerve group ( $14927 \pm 5089$  and  $6.04 \pm 0.85 \mu\text{m}$ ) than the silicon group ( $7429 \pm 1465$  and  $4.36 \pm 0.21 \mu\text{m}$ ). No tumors were observed in any of the rats in the Bio3D group at 24 weeks after surgery.

The Bio3D group showed significantly better nerve regeneration and there was no significant difference between the Bio3D group and the nerve autograft group in all endpoints.

## Keywords

peripheral nerve, nerve regeneration, nerve conduit, bio 3D printer

## Introduction

Peripheral nerve regeneration for long nerve defects is the most challenging aspect of the treatment of peripheral nerve injury, and numerous studies employing various approaches have been undertaken<sup>1–4</sup>. At present, the gold standard for the treatment of peripheral nerve injuries with defects is autologous nerve transplantation, but there are problems related to the comorbidities of donor sites, including numbness and pain at the harvested site, mismatch in the diameter between the recipient and the donor nerve, and the limitations in the length and number of nerves that can be harvested<sup>5–8</sup>. Various treatment methods have thus been

<sup>1</sup> Department of Orthopaedic Surgery, Kyoto University Graduate School of Medicine, Kyoto, Japan

<sup>2</sup> Department of Physical Therapy, Human Health Sciences, Graduate School of Medicine, Kyoto University, Kyoto, Japan

<sup>3</sup> Department of Regenerative Medicine and Biomedical Engineering, Saga University, Saga, Japan

<sup>4</sup> Cyfuse Biomedical K.K., Tokyo, Japan

Submitted: March 13, 2021. Revised: May 10, 2021. Accepted: May 11, 2021.

### Corresponding Author:

Ryosuke Ikeguchi, Department of Orthopaedic Surgery, Kyoto University Graduate School of Medicine, Kyoto, Japan.  
Email: [ikeguchir@me.com](mailto:ikeguchir@me.com)



developed to replace autologous nerve transplantation in the treatment of peripheral nerve injury.

In recent years, various organs and tissues have been developed using Bio3D printers<sup>9–11</sup>. In previous studies, we developed Bio3D conduits by fabricating cell spheroids made from various cells using a bio3D printer—this process is called the Kenzan method<sup>12</sup>. We previously reported the efficacy of sciatic nerve regeneration with defects in rat sciatic nerve models using Bio3D conduits made from human fibroblasts<sup>12</sup>. Using the Bio3D printer, we can determine the cell type, the so-called “Bio ink”<sup>13</sup>, and can also design the length, thickness, and diameter. In addition, this method is advantageous because the Bio 3D conduit is composed only of cells without artificial materials, so no problems related to foreign body reactions will arise. Furthermore, as the conduit will survive or will degenerate over time *in vivo*, it does not need to be removed afterwards<sup>14</sup>. Our previous study showed significantly better results for most evaluation parameters than the silicon group<sup>12</sup>. The follow-up period was as short as 8 weeks, however, which was not sufficiently long to confirm the progress of peripheral nerve regeneration. In the current study we conducted a long-term follow-up of 24 weeks to evaluate the nerve regeneration outcomes. In addition to the silicon group, we also compared the results with the autologous nerve transplantation group in this study, which is the current gold standard for the treatment of peripheral nerve injury. Bio3D conduit is composed solely of cells, which survive in the regenerated nerve. There is a possibility that the surviving cells could induce adverse events such as tumor genesis. An examination of adverse events over a long-term period is needed.

The purpose of this study was to evaluate the efficacy and safety of the Bio3D conduit made of human fibroblasts in peripheral nerve regeneration in the rat sciatic nerve model in a long-term follow-up of 24 weeks, and to compare the outcome with those of the groups treated by silicon tubes and autologous nerve grafting.

## Materials and Methods

### Creating Bio3D Conduit

We purchased cells of normal human dermal fibroblasts (NHDF) (Cat No. CC-2509) and NHDF medium composed of fibroblast basal medium (FBM) with fibroblast growth supplements (FGM-2) (Cat No. CC-3132) from Clonetics (Lonza, Walkersville, MD, USA), and the cells were expanded in the medium. Cells were passaged every 4 days, and the cells at passage 5 or 6 were used in this study.

Conduits were fabricated from NHDF using a Bio-3D printer (Regenova1, Cyfuse, Tokyo, Japan) employing the methods described by Ito et al.<sup>15</sup>. Briefly, cells detached with trypsin treatment were centrifuged, and the number of cells in the suspension was counted. The cells were re-suspended

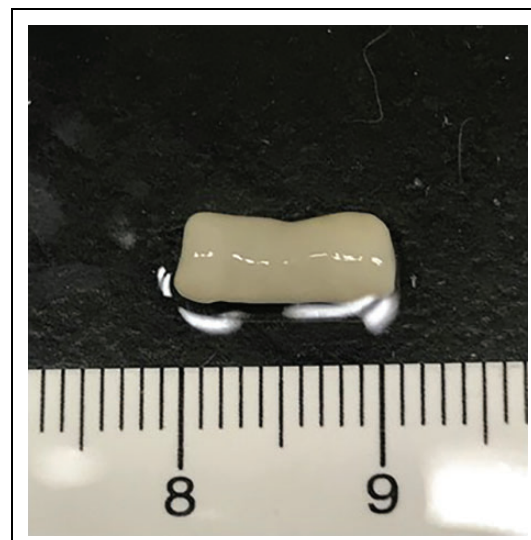


**Figure 1.** Bio3D conduit fabricated from normal human dermal fibroblasts. They were cultured in intravenous catheters until sufficient maturation. Bio3D conduit before the transplantation.

in a concentration of  $3 \times 10^5$  cells/mL and incubated in a low cell adhesion 96-well plate (SUMILON PrimeSurface1, Sumitomo Bakelite, Tokyo, Japan) for 24 h. Cells aggregated to form multicellular clusters called spheroids, and the diameter of each spheroid was approximately  $750 \pm 50 \mu\text{m}$ . Using the Bio3D printer, the spheroids were aspirated into the nozzle from each well and placed into needles arrayed in a circle as designed in advance, layer by layer. This Kenzan method allows the fabrication of three-dimensional (3D) structures according to pre-designed patterns. Approximately 1 week after printing, adjacent spheroids coalesced to create a Bio3D conduit in the needle array. The Bio3D conduit was removed from the needle array and transferred to an 18-gauge intravenous catheter (SURFLO: NIPRO, Osaka, Japan). The conduit culture was continued in a perfusion bioreactor until the desired function and strength were achieved. The inner diameter of the Bio3D conduit was 2 mm, with a wall thickness of  $500 \mu\text{m}$  (Fig. 1).

### Experimental Design

Fifteen adult F344 rnu-/rnu- male rats (9–10 weeks old; weighing 210–240 g, CLEA, Tokyo, Japan) that were partially immune deficient were used for this study. Rats were housed in flat-bottomed cages in pathogen-free rooms with unlimited food and water. They were randomly divided into three groups: the Bio3D group ( $n = 5$ ), the silicon group ( $n = 5$ ), and the nerve autograft group ( $n = 5$ ).

### Transplantation

Surgeries were performed on the right sciatic nerve of the rats under general anesthesia with isoflurane inhalation

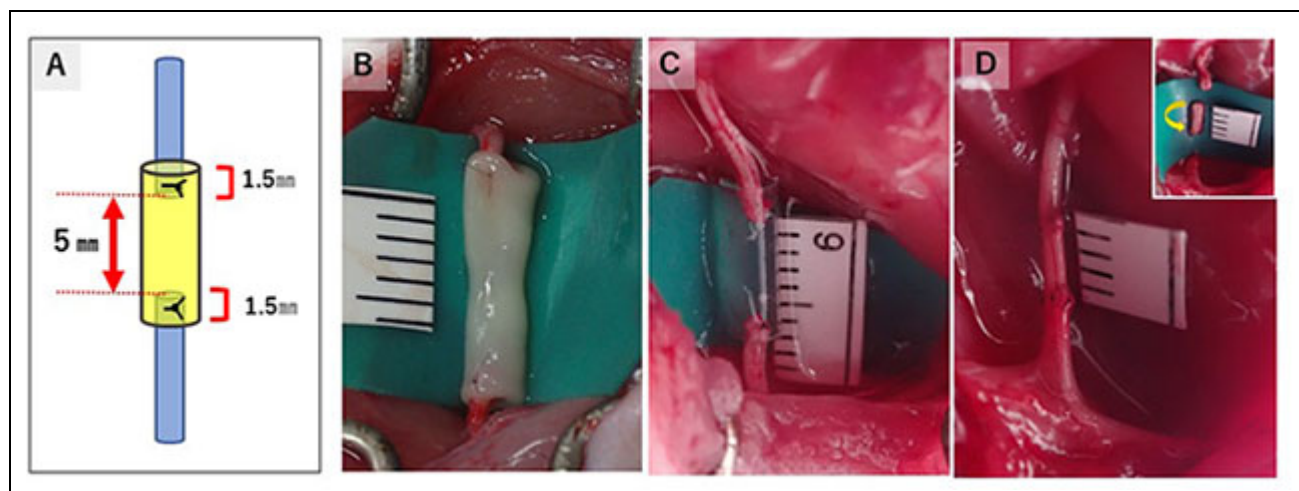


**Figure 2.** Reconstruction of a 5 mm nerve gap with three different methods and its schema. The schema illustrates the way of making a 5 mm nerve gap in the Bio3D group and the silicon group. The proximal stump and distal stump of the sciatic nerve was pulled 1.5 mm into the conduits in the (B) Bio3D group and the (C) silicon group. (D) In the nerve autograft group, the 5-mm-long sciatic nerve was removed and flipped to suture.

anesthesia. With the rat in the prone position, a skin incision was made from the lesion posterior to the greater trochanter to the popliteal fossa in the right hind limb, the fascia of the gluteal muscle was incised, and the muscle was split to expose the sciatic nerve. The right sciatic nerve was dissected in the middle of the thigh.

In the Bio3D group, a 5 mm gap was created in the mid-portion of the right sciatic nerve by cutting the nerve, and an 8-mm-long Bio3D conduit was transplanted between the proximal and distal stumps of the sciatic nerve. Both stumps were pulled in 1.5 mm each into the conduit to create a 5 mm gap between the nerve stumps. Both proximal and distal stumps of the nerve were anchored with 10-0 nylon suture under the operative microscope (Fig. 2). In the silicon group, an 8-mm-long silicon conduit was interposed with a 5 mm nerve gap using the same method. In the nerve autograft group, the right sciatic nerve was exposed in the same way as in the other two groups; 5 mm of the nerve was excised, and the proximal and distal stumps were flipped. Both stumps of the nerve segment were sutured with the sciatic nerve using 10-0 nylon suture. In all groups, the wound was closed in layers with 5-0 nylon suture. No external fixation was performed after the operation.

## Evaluation

### Pinprick Test/Toe-Spread Test

At 12, 16, 20, and 24 weeks, we evaluated the functional recovery of sensory nerves and motor nerves by the pinprick test and the toe-spread test, respectively. These tests were classified by Siemionow et al. and the results were scored as grade 0 to 3<sup>16</sup>.

In the pinprick test, the recovery of tactile and pain sensation was evaluated by the rat's reaction to being pinched on

its foot using forceps. Grade 0 indicates no response to stimulus, grade 1 indicates withdrawal of the foot following stimulus to the heel, grade 2 indicates withdrawal of the foot following stimulus to the dorsum of the foot, and grade 3 indicates withdrawal of the foot following stimulus to the toe. Better recovery is demonstrated as the grade moves from 0 to 3.

The toe-spread test is a method used to evaluate motor functional recovery. When a rat is suspended by the tail, the toes are normally abducted and hyperextended. If paralysis of the sciatic nerve exists, however, this does not occur. In grade 0, there is no toe reaction, grade 1 involves slight movement of the toes, grade 2 involves abduction of the toes, and grade 3 involves abduction and extension of the toes. Better recovery is demonstrated as the grade goes from 0 to 3.

### Kinematic Analysis

At 24 weeks after surgery, kinematic analysis using a treadmill was performed. With the rat in the prone position, colored hemispheric plastic markers were attached to five points and ink was applied on each joint of the hind limbs bilaterally. The five points included the anterior superior iliac spine, trochanter major joint of the hip, knee joint, lateral malleolus, and fifth metatarsophalangeal joint (MTP). In addition to the five markers, the toes were painted with acrylic resin ink for marking because the spheric plastic markers on the toe could be an obstacle for walking and the toes have very limited area to attach markers to.

Treadmill walking was recorded for a 3D kinematic analyzing system (Kinema Tracer System, Kissei Comtec, Nagano, Japan) by tracking each marker during walking. We evaluated two parameters: (1) drag toe (DT), which was the percentage of the step that was not off the ground during

walking, and (2) angle of attack (AoA), which was the angle between the toe and the metatarsal bone (made by the toe and the metatarsal) just before the toe touched the ground at the end of the swing phase. Smaller DT values and larger AoA values indicate better walking.

### Electrophysiological Study

Following kinematic analysis, electromyogram (EMG) examination was performed to measure the compound motor action potential (CMAP) and motor nerve conduction velocity (MNCV) of the pedal adductor muscles of the rats, which are innervated by the sciatic nerves. Under inhalation (general) anesthesia with isoflurane, using a needle electromyogram measuring system (Neuropack S1, MEB-9404, NIHON KOHDEN, Tokyo, Japan), stimulation electrodes were inserted into the point just behind the greater trochanter (S1) and popliteal fossa (S2) to stimulate the affected sciatic nerve, and a pair of electrodes was inserted into the pedal adductor muscle to obtain EMGs. The CMAP (mV) was obtained by measuring the height (peak to peak) of the EMG waveform evoked by stimulation of the S1 point. The MNCV (m/s) was calculated by dividing the accurate distance (mm) between the S1 and S2 points by the difference in latency (ms) between two EMG waveforms evoked by stimulating the S1 and S2 points. The same procedure was performed on the healthy side, and the percentage of the value of the affected side to the healthy side was calculated.

### Macroscopic Observation

Following the EMG examination, skin incisions were made in the same location as the previous operation and the right sciatic nerves were exposed to observe the changes in the surgical sites macroscopically and check nerve regeneration and tumor genesis.

### Wet Muscle Weight of the Tibialis Anterior Muscle

Following macroscopic observation, the tibialis anterior muscles, which are innervated by the sciatic nerve, of the operated side and the healthy side were dissected and harvested. We measured the wet weight of the whole muscle immediately using a digital scale. We evaluated the ratio of the wet muscle weight of the operated side to that of the healthy side. Larger values indicate better regeneration (and reinnervation) of the sciatic nerve, which prevents atrophy of the tibialis anterior muscle.

## Morphological Evaluation

### Number of Regenerated Myelinated Axons

The mid portions of the regenerative sciatic nerves of the operated side, 2.5 mm distal to the proximal nylon sutures for anchoring, were harvested and fixed with 1% glutaraldehyde and 1.44% paraformaldehyde in all three groups. Next,

the samples were fixed in 1% osmic acid and embedded in epoxy resin so pieces could be cut out transversely with a thickness of 1  $\mu$ m. They were then stained with 0.5% (w/v) toluidine blue solution and examined using a light microscope at a magnification of 400x (BZ-X700; KEYENCE, Osaka, Japan). We counted the total number of myelinated axons in the entire neural area in each sample using ImageJ software (National Institutes of Health, Bethesda, MD, USA).

### Myelinated Axon Diameter, Myelin Thickness, and Other Parameters

We analyzed additional properties of the regenerated myelinated axons using an ultra-thin section (1  $\mu$ m) obtained from the same sample as that used to evaluate the number of total myelinated axons in each sample of the three groups. The ultra-thin transverse sections (1  $\mu$ m) of each of the five samples from three groups were stained with lead citrate and uranyl acetate and examined using a transmission electron microscope (TEM; model H-7000, Hitachi High-Technologies, Tokyo, Japan) at a magnification of 2000 $\times$ . For more than 20% of the entire neural area of each sample, 6 or 7 randomly selected visual fields were photographed at a magnification of 2000 $\times$  in each sample of the three groups. We measured the following parameters using ImageJ software in 6 to 7 fields. The shortest myelinated axon diameter (a) and bare axon diameter (b) were measured. From these two measured values, myelin sheath thickness ( $[a-b] / 2$ ) and G-ratio ( $b / a$ ), which is the ratio of axon diameter to myelinated axon diameter, were calculated in each field. The mean values of the four parameters were calculated in each field, and from these results we obtained the mean values in all view fields (6–7 view fields) in each sample of the three groups.

### Immunohistochemistry

Immunohistochemical staining was performed on samples from each group to confirm nerve regeneration. After fixation with 4% PFA, samples cryoprotected with 20% saccharose solution were embedded with OCT compound to prepare for frozen sectioning. The frozen samples were cut into transverse and longitudinal sections with a thickness of 14  $\mu$ m and embedded on slide glasses. These prepared samples were washed with phosphate-buffered saline (PBS), and antigen retrieval was performed by proteinase K (Sigma-Aldrich, St. Louis, MO, USA) at room temperature for 15 min. For blocking, donkey serum was added on the slides and incubated at room temperature for 1 h, and then the primary antibodies, including rabbit polyclonal anti-S100 protein antibody (1:1000, Dako Carpinteria, CA, USA) used as a marker for Schwann cells, and mouse monoclonal anti-neurofilament H(NF-200) antibody (1:50, Abcam, Tokyo, Japan) used as a marker for neurofilament, were added and incubated at 4°C for 24 hours. The slides were washed with

**Table 1.** Results of the Pinprick Test for Evaluation of Sensory Recovery and the Toe-Spread Test for Evaluation of Motor Recovery at 24 Weeks After Surgery.

No.	Bio3D					Silicon					Autograft				
	#1	#2	#3	#4	#5	#1	#2	#3	#4	#5	#1	#2	#3	#4	#5
Pinprick	3	3	3	3	3	3	3	3	3	3	3	3	3	3	3
Toe-spread	3	3	3	3	3	2	2	3	3	3	3	3	3	3	3

In the Bio3D group and the autograft group, all rats scored grade 3 in both tests except for 2 of 5 rats who scored grade 2 in the toe-spread test in the silicon group.

PBS and incubated with secondary antibody (donkey anti-rabbit IgG [H + L], CFTM543 antibody, Sigma-Aldrich; donkey anti-mouse IgG [H + L], CFTM488 antibody, Sigma-Aldrich) for 1 h at room temperature. After washing with PBS, cover glasses were mounted on the slides using Fluoro-KEEPER anti-fade reagent, non-hardening type with DAPI (Nacalai Tesque, Kyoto, Japan). We also prepared the slides for negative control to determine the exposure time to exclude non-specific findings. We viewed and evaluated these slides using a confocal microscope (BZ-X700; KEYENCE, Osaka, Japan).

### Statistical Analyses

Regarding sample size, we sought to identify significant differences in histological and morphological study in this study based on our previous studies, and then performed a sample size analysis using statistical analysis software ( $\alpha = 0.05$ , power = 0.8; JMP pro software version 15.10.0; SAS Institute Inc., Cary, NC, USA). Five rats from each group were needed to detect a significant difference in those items.

The data were presented as values of the means and standard deviations. Data from kinematic analysis and electrophysiological study, the values of the wet muscle weight measurement, the number of myelinated axons and their measured properties such as the diameter of the axon and myelinated axon, myelin thickness, and G-ratio were compared using one-way analysis of variance, and a post hoc test was applied using the Tukey–Kramer test (JMP pro software version 15.10.0; SAS Institute Inc., Cary, NC, USA). The values were considered statistically significant at  $P < .05$  in all data.

## Results

### Pinprick Test/Toe-Spread Test

Regarding the pinprick test, three rats were grade 3 and two were grade 2 at 12 weeks in the Bio3D group. All five rats were grade 3 after 16 weeks in the Bio3D group. All rats in both the silicon group and the nerve autograft group were grade 3 at 12 weeks after surgery. There was no significant difference among the three groups at any of the time points, however. The results of the pinprick test at 24 weeks after surgery are shown in Table 1.

The toe-spread test had the same results in the Bio3D group and the nerve autograft group. Three rats were grade 3 and two were grade 2 at 12 weeks in the Bio3D group and in the nerve autograft group. At 16 weeks, the score was grade 3 in four rats and grade 2 in one rat. At 20 weeks after surgery in both groups, all rats were grade 3. In the silicon group, three rats were grade 3, one rat was grade 2, and one rat was grade 1 at 12, 16, and 20 weeks. At 24 weeks, three rats were grade 3 and two rats were grade 2 in the silicon group. The results at 24 weeks after surgery in the three groups are shown in Table 1.

### Kinematic Analysis

Mean DT was  $0.2 \pm 0.28$  in the Bio3D group,  $0.6 \pm 0.24$  in the silicon group, and  $0.16 \pm 0.18$  in the nerve autograft group (Fig. 3). Mean DT of the Bio3D group and the autograft group was significantly lower than that of the silicon group ( $P < .05$ ), and there was no significant difference between the two groups.

The mean AoA value was  $-20.67 \pm 10.94^\circ$  in the Bio3D group,  $-38.33 \pm 17.08^\circ$  in the silicon group, and  $-14.85 \pm 8.34^\circ$  in the nerve autograft group, respectively. The mean AoA value in the nerve autograft group was significantly better than that in the silicon group ( $P = .0357$ ), and there was no significant difference between the Bio3D group and the nerve autograft group.

### Electrophysiology Study

Twenty-four weeks after surgery, the mean ratio of the CMAP of the pedal adductor muscle was  $65.37\% \pm 7.57\%$  in the Bio3D group,  $53.86\% \pm 19.51\%$  in the silicon group, and  $85.13\% \pm 6.46\%$  in the nerve autograft group (Fig. 4). The nerve autograft group showed significantly better recovery in the CMAP than the silicon group ( $P < .01$ ). There was no significant difference between the Bio3D group and the nerve autograft group. As for the MNCV, the mean values were  $48.97\% \pm 19.19\%$  in the Bio3D group,  $61.36\% \pm 25.18\%$  in the silicon group, and  $54.17\% \pm 11.89\%$  in the nerve autograft group. There was no significant difference among the three groups.

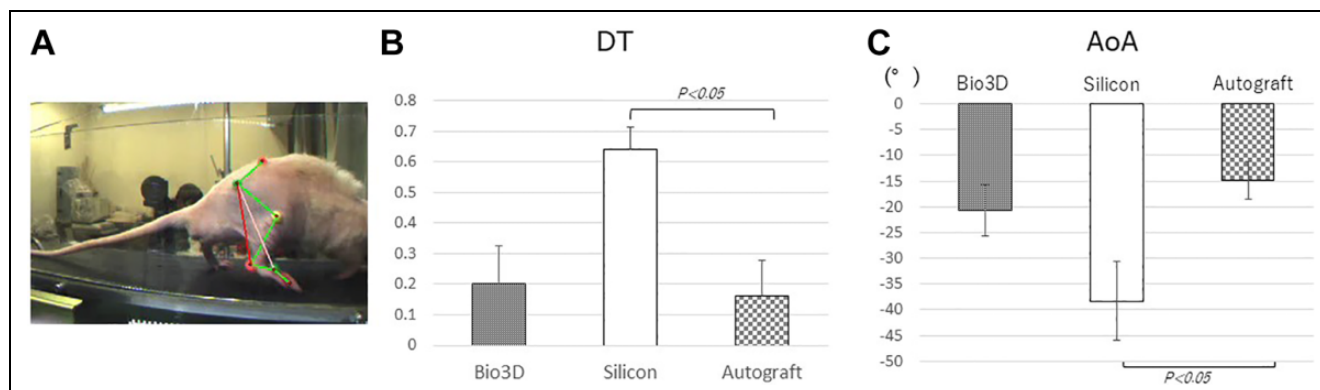


**Figure 3.** Results of kinematic analysis. (A) Measurement of the AoA using the kinematic analysis system by tracking each marker to measure the angle between the metatarsal bone and the toe just before toe-touch. (B) The DT, which represents the ratio of dragging during continuous steps, was significantly higher in the silicon group than the other two groups. (C) Although the AoA, which represents the degree of dropped toe, tended to be better in the Bio3D group and the autograft group, a significant difference was only observed between the silicon group and the autograft group ( $P < .05$ ).

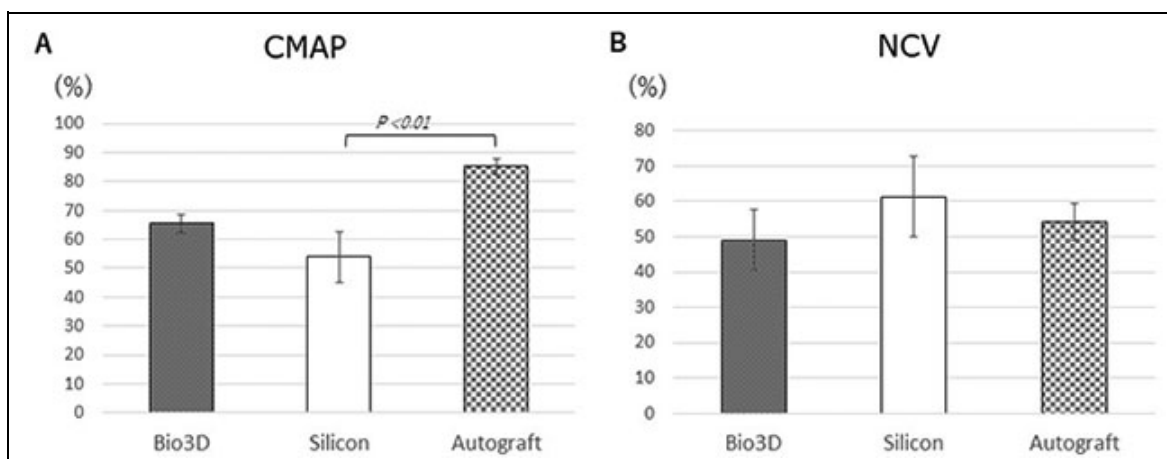


**Figure 4.** Results of electrophysiological evaluation for the target muscle of the sciatic nerve. (A) The mean recovery of the CMAP was better in the Bio3D group ( $65.37\% \pm 7.57\%$ ) and the nerve autograft group ( $85.13\% \pm 6.46\%$ ) than in the silicon group ( $53.86\% \pm 19.51\%$ ), although there was only a significant difference between the silicon group and the autograft group ( $P < .01$ ). (B) As for the NCV, there was no significant difference among the three groups.

### Macroscopic Observation

We observed the changes in the transplantation sites of the sciatic nerve in each group at 24 weeks post-operation (Fig. 5). In all of the rats in the three groups, the dissected sciatic nerves were successfully bridged. All of the Bio3D conduits had larger diameters compared to the sciatic nerves at the time of transplantation surgery. After 24 weeks, the thickness was the same as the sciatic nerves, and no tumor formation, including neuromas, was observed in any of the rats. In the silicon group, all regenerated nerves in the silicon tubes were thinner than both the normal sciatic nerves and the diameter of the tubes.

### Wet Muscle Weight of the Tibialis Anterior Muscle

The mean ratio of the wet weight of the tibialis anterior muscle, the innervated muscle of the sciatic nerve, was

$79.85\% \pm 5.47\%$  in the Bio3D group,  $66.99\% \pm 3.51\%$  in the silicon group, and  $81.74\% \pm 2.83\%$  in the nerve autograft group (Fig. 6). The values were significantly larger in both the Bio3D group and the nerve autograft group than in the silicon group ( $P < .05$ ), and there was no significant difference between the Bio3D group and the nerve autograft group.

### Morphological Evaluation

The number of myelinated axons was  $14708 \pm 3021$  in the Bio3D group,  $7429 \pm 1465$  in the silicon group, and  $14927 \pm 5089$  in the nerve autograft group (Fig. 7). The Bio3D group and the nerve autograft group had a significantly larger number of myelinated axons than the silicon group ( $P = .0126$ ,  $P = .018$ , respectively). There was

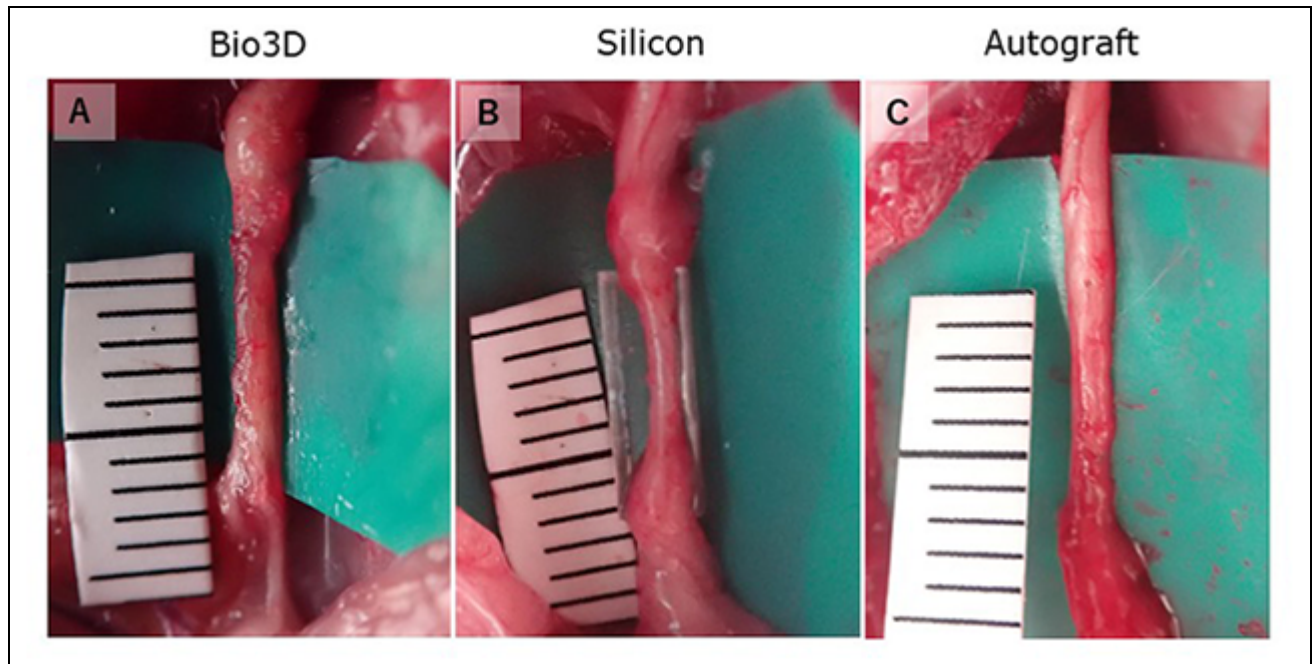


**Figure 5.** Macroscopic observation of the transplanted sites 24 weeks after surgery (A–C). (A) The Bio3D conduit was degenerated and regenerated nerve was observed. (B) The regenerated nerve was thin in the silicon tube. (C) Regenerated nerve was observed in the autograft group.

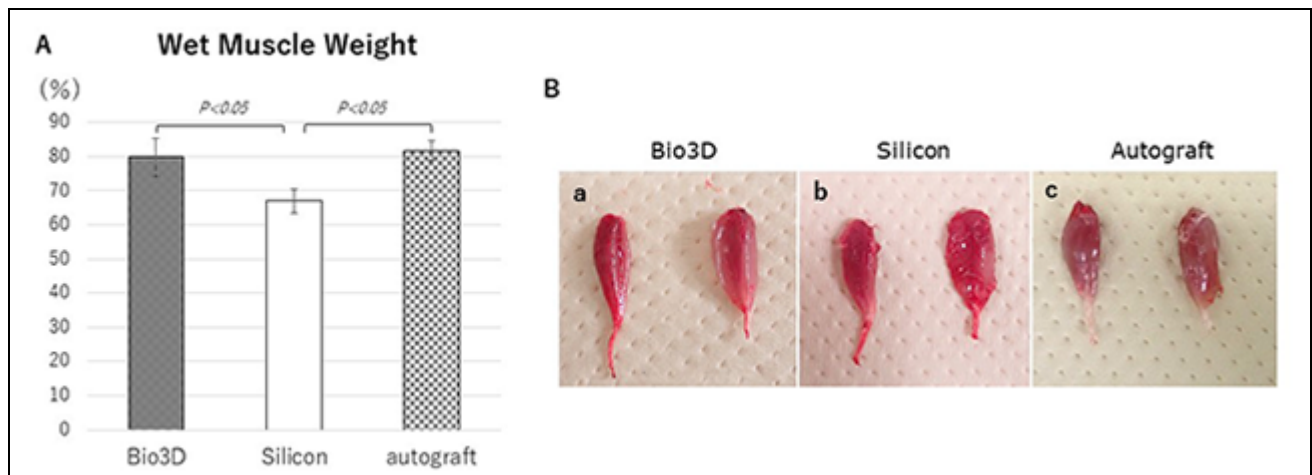


**Figure 6.** Wet muscle weight of the tibial anterior muscle. (A) Little muscle atrophy was observed in the Bio3D group ( $79.85\% \pm 5.47\%$ ) and the autograft group ( $81.74\% \pm 2.83\%$ ) compared with the silicon group ( $66.99\% \pm 3.51\%$ ). (B) The whole appearance of the dissected tibial anterior muscles of (a) the Bio3D group, (b) the silicon group, and (c) the autograft group.

no significant difference between the Bio3D group and the autograft group.

The mean diameter of myelinated axons was  $5.52 \pm 0.44 \mu\text{m}$  in the Bio3D group,  $4.36 \pm 0.21 \mu\text{m}$  in the silicon group, and  $6.04 \pm 0.84 \mu\text{m}$  in the nerve autograft group (Fig. 8). The mean diameters of myelinated axons in the Bio3D group and the nerve autograft group were significantly larger than that in the silicon group ( $P = .0123$ ,  $P = .00009$ , respectively), and there was no significant difference between the Bio3D group and the nerve autograft group.

The mean diameter of axons was  $3.58 \pm 0.28 \mu\text{m}$  in the Bio3D group,  $3.04 \pm 0.24 \mu\text{m}$  in the silicon group, and  $3.9 \pm 0.55 \mu\text{m}$  in the nerve autograft group. There was a significant difference between the silicon group and the nerve autograft groups ( $P < .01$ ).

The mean myelin thickness was  $0.97 \pm 0.08 \mu\text{m}$  in the Bio3D group,  $0.66 \pm 0.08 \mu\text{m}$  in the silicon group, and  $1.07 \pm 0.19 \mu\text{m}$  in the nerve autograft group. The values of the Bio3D group and the nerve autograft group were significantly larger than that in the silicon group ( $P = .0049$  and



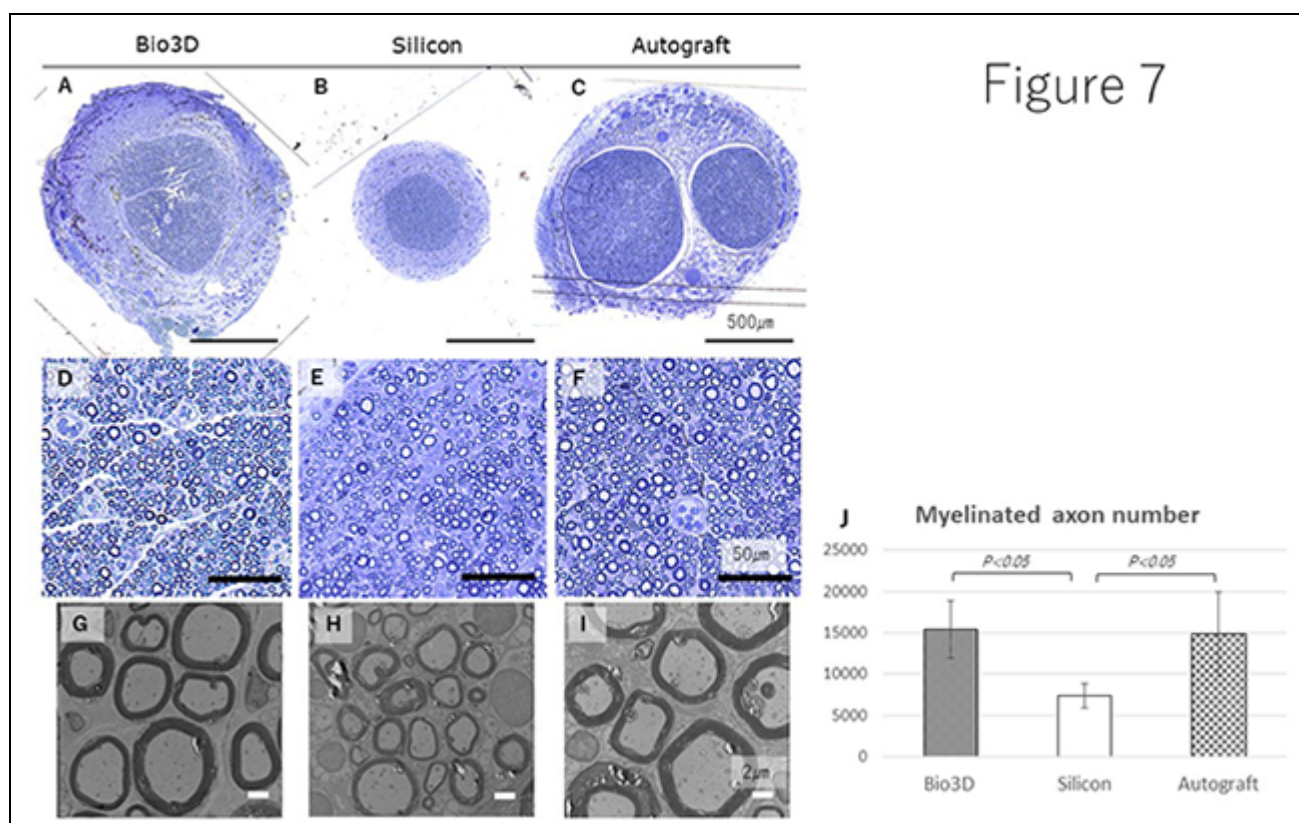


**Figure 7.** (A–I) Histology of the mid-portion regenerated nerves and (J) myelinated axon number of the middle portion of the regenerated sciatic nerve. (A–F) Semi-thin transverse sections stained with toluidine blue at different magnifications. (G–I) Ultra-thin transverse sections observed with transmission electron microscopy. Whole images of the specimens show that the regenerated nerves of the silicon group (B) were smaller than those of the Bio3D group (A) and the autograft group (C). Magnified images of semi-thin (D–F) and ultra-thin transverse sections (G–I) revealed that myelinated axons with larger diameter and thicker myelin sheath were regenerated in the Bio3D group and the autograft group than in the silicon group. (J) Myelinated axon number of the middle portion of regenerated sciatic nerve. The Bio3D group ( $14708 \pm 3021$ ) and autograft group ( $14927 \pm 5089$ ) showed a significantly greater number than the silicon group ( $7429 \pm 1465$ ), and there was no significant difference between the two groups.

$P = .0006$ , respectively), and there was no significant difference between the Bio3D group and the nerve autograft group.

The mean value of the G-ratio was  $0.63 \pm 0.02$  in the Bio3D group,  $0.69 \pm 0.04$  in the silicon group, and  $0.63 \pm 0.02$  in the nerve autograft group. There were significantly smaller values in the Bio3D group and the nerve autograft group than in the silicon group ( $P = .0224$ ,  $P = .0204$ , respectively), and there was no significant difference between the Bio3D group and the nerve autograft group.

### Immunohistochemistry

Immunohistochemical examination in all groups demonstrated the expression of S-100 and NF-200 with DAPI in the mid portion of the regenerated nerve (Fig. 9). These results revealed the existence of Schwann cells and neural fibers in the sites where the defects between the proximal and the distal stumps of the dissected sciatic nerves were bridged by the Bio3D conduits, silicon tube, and nerve autograft.

### Discussion

In our previous study, the outcomes of the Bio3D conduit were greater than those of the silicon tube in many parameters of the evaluation<sup>12</sup>. The CMAP of the target muscles, number of regenerated axons, wet weight of the target muscles, and AoA values in kinematic analysis showed significantly better results than those of the silicon group<sup>12</sup>. There was no significant difference in other parameters between the Bio3D group and the silicon group, however.

In this long-term follow-up study, the number of regenerated axons in the Bio3D group was also significantly larger than that of the silicon group, and the myelinated axon diameter, myelin thickness, and G-ratio also showed significantly greater results in the Bio3D group. These outcomes were not significantly different than those of the autologous nerve group. This means that the maturation and myelination of the regenerated nerve in the Bio3D group progressed more than those in the silicon group and were similar to those in the autologous nerve group over the long-term period of 24 weeks. These results are consistent with those of the wet

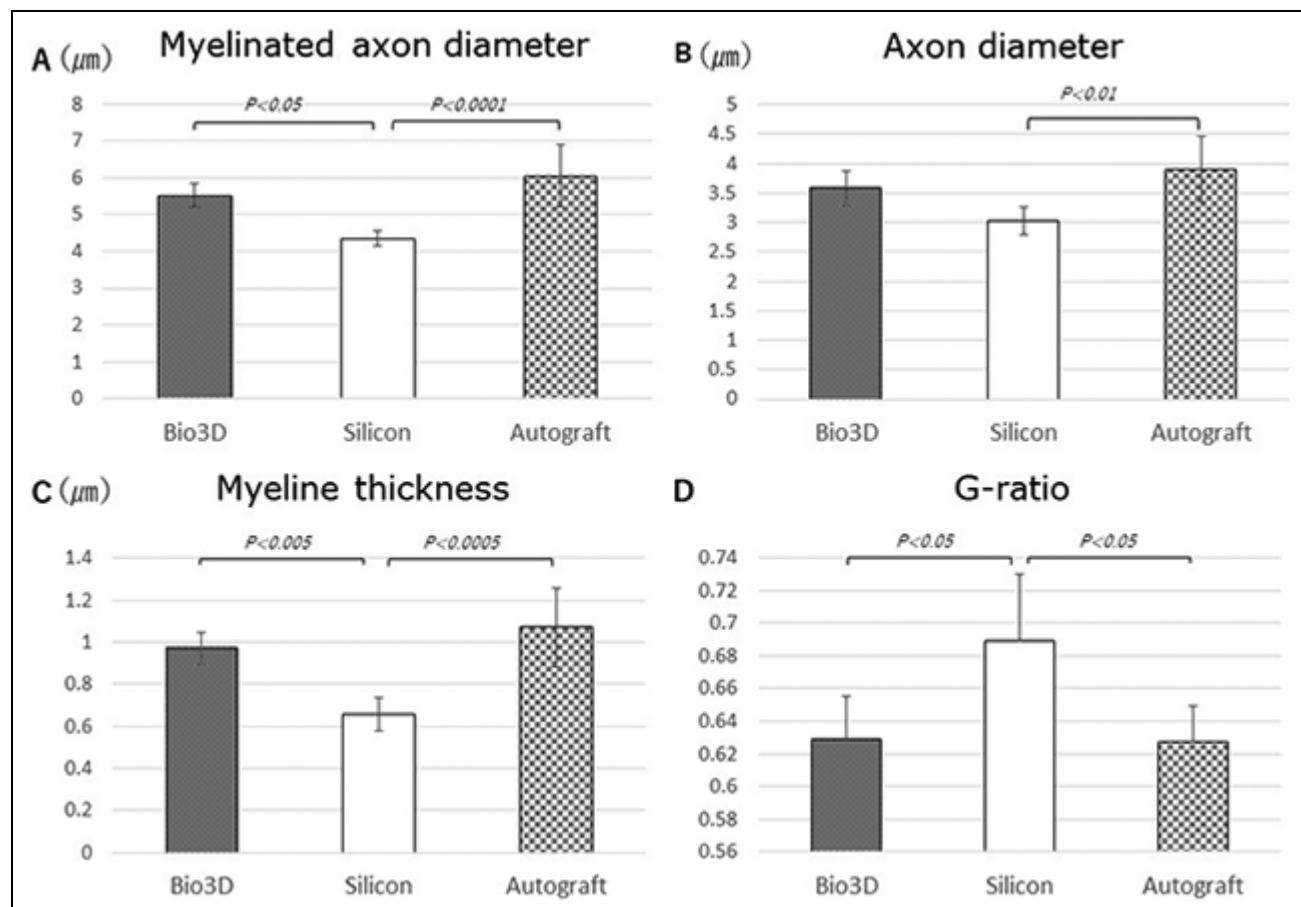


**Figure 8.** Morphological evaluations of the myelinated axon. (A) The mean myelinated axon diameter of both the Bio3D group ( $5.52 \pm 0.44 \mu\text{m}$ ) and the autograft group ( $6.04 \pm 0.84 \mu\text{m}$ ) was significantly larger than that of the silicon group ( $4.36 \pm 0.21 \mu\text{m}$ ). (B) The mean axon diameter of the autograft group ( $3.9 \pm 0.55 \mu\text{m}$ ) was significantly larger than that of the silicon group ( $3.04 \pm 0.24 \mu\text{m}$ ) although there was no significant difference between it and the Bio3D group ( $3.58 \pm 0.28 \mu\text{m}$ ). (C) Myelin sheath was significantly thicker in the Bio3D group ( $0.97 \pm 0.08 \mu\text{m}$ ) and the autograft group ( $1.07 \pm 0.19 \mu\text{m}$ ) than in the silicon group ( $0.66 \pm 0.08 \mu\text{m}$ ). (D) The mean G-ratio was significantly lower in the Bio3D group ( $0.63 \pm 0.02$ ) and the autograft group ( $0.63 \pm 0.02$ ) than in the silicon group ( $0.69 \pm 0.04$ ).

muscle weight of the target muscle and DT in kinematic analysis in which the weight and DT in the Bio3D group were greater than that in the silicon group. As a result of sciatic nerve regeneration and the reinnervation into the target muscle, atrophy of the target muscle was prevented. In the immunohistochemical examination in which the images are generally unclear, all of the groups demonstrated expression of S-100 and NF-200 and morphological study showed significant differences in myelinated axon number, diameter, myelin thickness, and G-ratio. Against this background, we did not perform quantitative analysis of the immunohistochemical examination results.

In mean AoA values, another parameter of kinematic analysis, there was no significant difference between the Bio3D group and the silicon group. It is possible that DT (which presents the frequency of the DT) is more important than the AoA value (which presents the degree of the dropped toes just before loading of each step in actual gait). In addition, there were no differences in MNCV results among the three groups. MNCV results depend on the

existence of large myelinated axons. A small number of large myelinated axons leads to better MNCV results. As such, it is difficult to detect a significant difference among the groups in MNCV study.

As the material for bridging the defect between the peripheral nerve stumps, it is essential to maintain the luminal structure that provides a place for nerve regeneration and prevents the invasion of scars. At the same time, it is essential to allow blood flow and the permeability of growth factors, neurotrophic factors, and cytokines<sup>17,18</sup>. In the toluidine blue-stained specimen of the Bio3D group in the current study, numerous blood vessels were observed among regenerated axons, which implies that the Bio3D conduit retains permeability during the nerve regeneration period. We believe that these results demonstrate the efficacy of the treatment using Bio3D conduits for peripheral nerve injury with defect.

Nerve regeneration using Bio3D conduits can depend on the type of cells that compose the conduits. We have previously investigated which type of cell is most optimal for

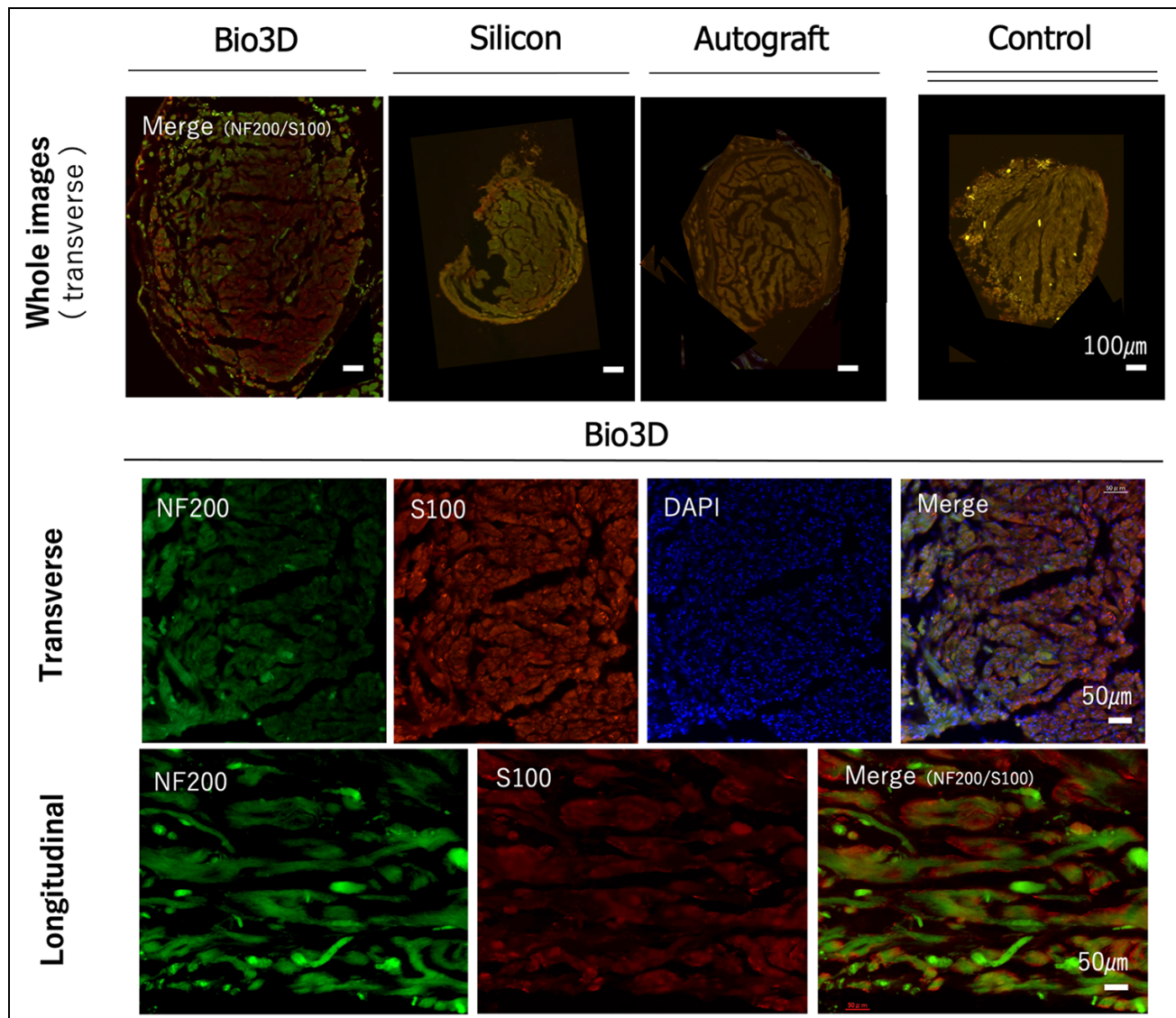


**Figure 9.** Immunohistochemistry of the middle portion of a regenerated sciatic nerve harvested from a rat in each of the three groups. The upper row shows overall images of the transverse section (scale bar indicates 100  $\mu$ m) in each of the three groups. Control is an intact sciatic nerve harvested from a healthy rat. The middle row shows magnified images of the transverse section (scale bar indicates 50  $\mu$ m), and the lower row shows magnified images of the longitudinal section (scale bar indicates 50  $\mu$ m) fluorescently stained by NF200, S-100, DAPI, and merged in the Bio3D group. An S-100-positive lesion can be observed around nerve fibers stained by NF200, which implies nerve regeneration at the middle portion of the sciatic nerve defect lesion bridged by a Bio3D conduit.

Bio3D conduits in peripheral nerve regeneration therapy. Focusing on the pluripotency, proliferative potential, and paracrine ability of mesenchymal stem cells (MSCs), we have conducted nerve regeneration studies using Bio3D conduit made from MSCs developed from iPS cells<sup>19</sup> and bone marrow MSCs<sup>20</sup>. As for cell type, both the outcomes of nerve regeneration and other aspects, such as cell harvesting difficulty, donor site morbidity, and easy cell handling, should be taken into consideration. The fibroblasts used in this study can be obtained from a small amount of skin, are easy to culture and proliferate, provide sufficient strength to maintain the luminal structure, and also offer good handling for suturing to nerve stumps. We previously reported the

high survival rate of the cells comprising the Bio3D conduits before and 1 week after transplantation in the same experimental model<sup>14</sup>. It was reported that fibroblasts promote the migration of Schwann cells to the injury site of the nerve<sup>21</sup>, and also promote the vascularization of tissue<sup>22,23</sup>, both of which have been shown to play an important role in the early stages of peripheral nerve repair. In addition, it was reported that fibroblasts can differentiate into Schwann-like cells<sup>24</sup>.

There are several limitations to this study. First, although the current study demonstrated good results in peripheral nerve regeneration, the number of rats used in this experiment was relatively small and the 5 mm defect length is not a critical gap. Furthermore, this study did not have a neurotmesis control

group in which the sciatic nerve of the rats was dissected with no repair. Our previous study employed a 10 mm sciatic nerve defect model in rats using Bio3D conduits made from human fibroblasts and demonstrated good nerve regeneration, however<sup>25</sup>. More cells are needed to create a 13 mm Bio3D conduit to a 10 mm nerve gap, and the purpose of the study is long-term follow-up of 24 weeks. In the current study we thus used a 5 mm nerve defect model. The silicon group had better nerve regeneration than the transected nerve without repair group, in which rats had no nerve regeneration. Given this, we compared nerve regeneration between the Bio3D group and the silicon group. Second, the confirmation of the safety of the Bio3D conduit made from human fibroblasts was insufficient. No obvious tumor formation was observed locally in all rats in the Bio3D group during the long-term follow-up of 24 weeks. Safety needs to be confirmed from multiple perspectives, however, such as blood analysis and the histological evaluation of other organs. A third limitation is that the autologous nerve graft method in the current study differs from that in clinical practice. In clinical practice, pure sensory nerves are used as donors for autologous nerve transplantation (sural nerve, etc.). In this experimental model, however, the autologous nerve graft that was resected from the sciatic nerve contains motor nerve segments. Motor nerve segment grafts are reported to show better nerve regeneration than sensory nerve grafts<sup>26,27</sup>. The current study model may thus show better motor function recovery results than in clinical practice. The difference between the results of the Bio3D group in this study and autologous transplantation in clinical practice might be smaller than this study. A fourth limitation is the lack of an evaluation of functional recovery over time. In the current study, we did not evaluate functional recovery over time in kinematic and electrophysiological analysis. General anesthesia is necessary for kinematic analysis and electrophysiological study. As such, we did not perform kinematic analysis or electrophysiological study at different points of the experiment except for the end point.

## Conclusions

We conducted a 24-week long-term follow-up study in a rat model with a 5 mm defect in the sciatic nerve using a Bio3D conduit fabricated from human fibroblasts. The safety and nerve regeneration was confirmed through both functional and histological evaluations.

## Ethical Approval

The experimental protocols were approved by the Animal Research Committee, Kyoto University Graduate School of Medicine.

## Statement of Human and Animal Rights

All animal studies were approved by the Animal Research Committee, Kyoto University Graduate School of Medicine and were performed according to the guidelines of the Animal Research Committee, Kyoto University Graduate School of Medicine.

## Statement of Informed Consent

There are no human subjects in this article and informed consent is not applicable.


## Declaration of Conflicting Interests


The author(s) declared no potential conflicts of interest with respect to the research, authorship, and/or publication of this article.

## Funding

The author(s) received no financial support for the research, authorship, and/or publication of this article.

## ORCID iD

Ryosuke Ikeguchi  <https://orcid.org/0000-0003-4525-7849>

Koichi Nakayama  <https://orcid.org/0000-0002-7324-8862>

## References

- Ni HC, Tseng TC, Chen JR, Hsu SH, Chiu IM. Fabrication of bioactive conduits containing the fibroblast growth factor 1 and neural stem cells for peripheral nerve regeneration across a 15 mm critical gap. *Biofabrication*. 2013;5(3):035010.
- Sayanagi J, Tanaka H, Ebara M, Okada K, Oka K, Murase T, Yoshikawa H. Combination of electrospun nanofiber sheet incorporating methylcobalamin and pga-collagen tube for treatment of a sciatic nerve defect in a rat model. *J Bone Joint Surg Am*. 2020;102(3):245–253.
- Fu KY, Dai LG, Chiu IM, Chen JR, Hsu SH. Sciatic nerve regeneration by microporous nerve conduits seeded with glial cell line-derived neurotrophic factor or brain-derived neurotrophic factor gene transfected neural stem cells. *Artif Organs*. 2011;35(4):363–372.
- Dai LG, Huang GS, Hsu SH. Sciatic nerve regeneration by cocultured Schwann cells and stem cells on microporous nerve conduits. *Cell Transplant*. 2013;22(11):2029–2039.
- Lundborg G. A. 25-year perspective of peripheral nerve surgery: evolving neuroscientific concepts and clinical significance. *J Hand Surg Am*. 2000;25(3):391–414.
- Hallgren A, Björkman A, Chemnitz A, Dahlin LB. Subjective outcome related to donor site morbidity after sural nerve graft harvesting: a survey in 41 patients. *BMC Surg*. 2013;13:39.
- Ijima FF, Nicolai JP, Meek MF. Sural nerve donor-site morbidity: thirty-four years of follow-up. *Ann Plast Surg*. 2006;57(4):391–395.
- Tada K, Nakada M, Matsuta M, Yamauchi D, Ikeda K, Tsuchiya H. Long-term outcomes of donor site morbidity after sural nerve graft harvesting. *J Hand Surg Global Online*. 2020;2(2):74–76.
- Critchley S, Sheehy EJ, Cunniffe G, Diaz-Payno P, Carroll SF, Jeon O, Alsberg E, Brama PAJ, Kelly DJ. 3D printing of fibre-reinforced cartilaginous templates for the regeneration of osteochondral defects. *Acta Biomater*. 2020;113:130–143.
- Dikina AD, Strobel HA, Lai BP, Rolle MW, Alsberg E. Engineered cartilaginous tubes for tracheal tissue replacement via self-assembly and fusion of human mesenchymal stem cell constructs. *Biomaterials*. 2015;52:452–462.

11. Hoch E, Tovar GE, Borchers K. Bioprinting of artificial blood vessels: Current approaches towards a demanding goal. *Eur J Cardiothorac Surg.* 2014;46(5):767–778.
12. Yurie H, Ikeguchi R, Aoyama T, Kaizawa Y, Tajino J, Ito A, Ohta S, Oda H, Takeuchi H, Akieda S, Tsuji M, et al. The efficacy of a scaffold-free Bio 3D conduit developed from human fibroblasts on peripheral nerve regeneration in a rat sciatic nerve model. *PLoS One.* 2017;12(2):e0171448.
13. Chung JHY, Naficy S, Yue Z, Kapsa R, Quigley A, Moulton SE, Wallace GG. Bio-ink properties and printability for extrusion printing living cells. *Biomater Sci.* 2013;1(7):63–773.
14. Yurie H, Ikeguchi R, Aoyama T, Ito A, Tanaka A, Noguchi T, Oda H, Takeuchi H, Mitsuzawa S, Ando M, Yoshimoto K, et al. Mechanism of peripheral nerve regeneration using a Bio 3D conduit derived from normal human dermal fibroblasts. *J Reconstr Microsurg.* 2020;37(4):357–364. doi:10.1055/s-0040-1716855. Online ahead of print
15. Itoh H, Nakayama K, Noguchi R, Kamohara K, Furukawa K, Uchiyama K, Toda S, Oyama J, Node K, Morita S. Scaffold-free tubular tissues created by a Bio-3D printer undergo remodeling and endothelialization when implanted in rat aortae. *PLoS One.* 2015;10(12):e0145971.
16. Siemionow M, Duggan W, Brzezicki G, Klimczak A, Grykien C, Gatherwright J, Nair D. Peripheral nerve defect repair with epineural tubes supported with bone marrow stromal cells: a preliminary report. *Ann Plast Surg.* 2011;67(1):73–84.
17. Chang CJ, Hsu SH. The effect of high outflow permeability in asymmetric poly(dl-lactic acid-co-glycolic acid) conduits for peripheral nerve regeneration. *Biomaterials.* 2006;27(7):1035–1042.
18. Kim DH, Connolly SE, Zhao S, Beuerman RW, Voorhies RM, Kline DG. Comparison of macropore, semipermeable, and nonpermeable collagen conduits in nerve repair. *J Reconstr Microsurg.* 1993;9(6):415–420.
19. Mitsuzawa S, Zhao C, Ikeguchi R, Aoyama T, Kamiya D, Ando M, Takeuchi H, Akieda S, Nakayama K, Matsuda S, Ikeya M. Pro angiogenic scaffold free bio three dimensional conduit developed from human induced pluripotent stem cell derived mesenchymal stem cells promotes peripheral nerve regeneration. *Sci Rep.* 2020;10(1):12034.
20. Yurie H, Ikeguchi R, Aoyama T, Tanaka M, Oda H, Takeuchi H, Mitsuzawa S, Ando M, Yoshimoto K, Noguchi T, Akieda S, et al. Bio 3D conduits derived from bone marrow stromal cells promote peripheral nerve regeneration. *Cell Transplant.* 2020;29:1–9.
21. Zhang Z, Yu B, Gu Y, Zhou S, Qian T, Wang Y, Ding G, Ding F, Gu X. Fibroblast-derived tenascin-C promotes Schwann cell migration through beta1-integrin dependent pathway during peripheral nerve regeneration. *Glia.* 2016;64(3):374–385.
22. Sorrell JM, Caplan AI. Fibroblasts—a diverse population at the center of it all. *Int Rev Cell Mol Biol.* 2009;276:161–214.
23. Dun XP, Parkinson DB. Classic axon guidance molecules control correct nerve bridge tissue formation and precise axon regeneration. *Neural Regen Res.* 2020;15(1):6–9.
24. Thoma EC, Merkl C, Heckel T, Haab R, Knoflach F, Nowaczyk C, Flint N, Jagasia R, Jensen Zoffmann S, Truong HH, et al. Chemical conversion of human fibroblasts into functional Schwann cells. *Stem Cell Rep.* 2014;3(4):539–547.
25. Takeuchi H, Ikeguchi R, Aoyama T, Oda H, Yurie H, Mitsuzawa S, Tanaka T, Ohta S, Akieda S, Miyazaki Y, Nakayama K, et al. A scaffold-free Bio 3D nerve conduit for repair of a 10-mm peripheral nerve defect in the rats. *Microsurgery.* 2020;40(2):207–210.
26. Brenner MJ, Hess JR, Myckatyn TM, Hayashi A, Hunter DA, Mackinnon SE. Repair of motor nerve gaps with sensory nerve inhibits regeneration in rats. *Laryngoscope.* 2006;116(9):1685–1692.
27. Moradzadeh A, Borschel GH, Luciano JP, Whitlock EL, Hayashi A, Hunter DA, Mackinnon SE. The impact of motor and sensory nerve architecture on nerve regeneration. *Exp Neurol.* 2008;212(2):370–376.